

## Analysis of Dynamic Fracture with Cohesive Crack Segment Method

H.X. Wang and S.X. Wang

**Abstract:** In the meshfree cohesive crack method, the discrete crack is modeled by a set of cohesive crack segments which can be arbitrarily oriented. Propagation of the crack is achieved by activation of crack surfaces at individual nodes, so no representation of the crack surface is needed. The crack is modeled by a local enrichment of the test and trial functions with sign function, so that discontinuities are along the direction of the crack. A set of cracking rules is developed to avoid spurious cracking.

**Keyword:** Computational Mechanics, Applied Mathematics, Fracture Mechanics, Applied Mechanics

### 1 Introduction

Besides the existence of numerous powerful computational methods for crack problems Ortiz, Leroy, and Needleman (1987); Belytschko and Lu (1995); Belytschko, Lu, and Gu (1995); Belytschko and Tabbara (1996); Belytschko and Fleming (1999); Macri and De (2008); Volokh (2004); Ostachowicz (2008), the simulation of a large set of evolving cracks by computational methods still poses substantial difficulties. The most pertinent difficulty is tracking the crack path that becomes especially cumbersome for a large set of evolving cracks. Meshfree methods are particularly suited for crack problems since they do not rely on a mesh that needs to be adjusted once a crack propagates. Meshfree methods especially emerged in the 90s. Most popular meshfree methods are the Meshless Local Petrov Galerkin (MLPG) method Atluri and Zhu (1998, 2000); Atluri and Shen (2002), the element-free Galerkin (EFG) method Belytschko, Lu, and Gu (1994a) and the Reproducing Kernel Particle Method (RKPM) Liu, Jun, and Zhang (1995). Besides of applications involving fracture, see e.g. Liu, Hao, and Belytschko (1999); Nishioka, Tchouikov, and Fujimoto (2006); Sladek, V. Sladek, and Zhang (2007); Rabczuk and Zi (2007); Rabczuk, PMA, and Belytschko (2007); Rabczuk and Belytschko (2007); Zi, Rabczuk, and Wall (2007); Hao, Liu, and Chang (2000); Hao, Liu, and

Qian (2000); Rabczuk, Areias, and Belytschko (2007); Chen and Chen (2005); Xu, Dong, and Zhang (2008); Hao, Liu, Klein, and Rosakis (2004); Wen, Aliabadi, and Lin (2008); Guo and Nairn (2006a); Rabczuk and Areias (2006a); Miers LS (2006); Gao, Liu, and Liu (2006a); Guo and Nairn (2006b); Ma, Lu, and Wang (2006); Fujimoto and Nishioka (2006); Chen, Gan, and Chen (2008); Nishioka (2005); Andreaus, Batra, and Porfiri (2005); Nairn (2003); Rabczuk and Belytschko (2006); Maiti and Geubelle (2004); Liu, Long, and Li (2008); ?, their advantages were exploited in various other applications in fluid and solid mechanics Idelsohn, Onate, and Pin (2004); Nishioka, Kobayashi, and Fujimoto (2007); Chen, Gan, and Chen (2008); Vavourakis and Polyzos (2007); Han and Atluri (2004); Nguyen-Van, N, and Tran-Cong (2008); Rabczuk, Belytschko, and Xiao (2004); Hao and Liu (2006); Guz, Menshykov, and Zozulya (2007); Mai-Duy, Khennane, and Tran-Cong (2007); Rabczuk and Areias (2006b); Wu and Liu (2007); Wen and Hon (2007); Wu and Tao (2007); Wu and Liu (2007); Sladek, Sladek, and Zhang (2007); Hagihara, Tsunori, and Ikeda (2007); Rabczuk and Belytschko (2005); Guo and Nairn (2006b); Fujimoto and Nishioka (2006); Gao, Liu, and Liu (2006b); Sladek, Sladek, and Krivacek (2005); Nishioka, Tchouikov, and Fujimoto (2006); Le, Mai-Duy, and Tran-Cong (2008); Liu, Long, and Li (2008). An excellent book of mesh-free methods is the one by Atluri (2002).

The visibility method Belytschko, Lu, and Gu (1994b) or improvements of the visibility method Organ, Fleming, Terry, and Belytschko (1996) are commonly used for problems involving cracks. Recently, level set methods have been used by some meshfree methods for crack problems Ventura, Xu, and Belytschko (2002). Though no remeshing is needed in meshfree methods, the need to track the crack path remains. Recently, meshfree methods were developed that do not need to track the crack path Rabczuk and Belytschko (2004, 2007). In these methods, the crack is modeled by a set of cracked nodes. These can be arbitrarily oriented, but the growth is represented discretely by activation of crack surfaces at individual nodes, so no representation of the crack surface is needed. The crack is modeled by a local enrichment of the test and trial functions with a sign function, so that the discontinuities are along the direction of the crack. The discontinuity consists of cohesive crack segments that pass through the entire domain of influence at the node. One major advantage of the method is that it can handle crack propagation and crack nucleation in the same manner. However, the approach presented in Rabczuk and Belytschko (2004) often leads to spurious cracking adjacent to existing crack and henceforth to an overestimation of the cohesive fracture energy similar to interface elements Ortiz, Leroy, and Needleman (1987); Xu and Needleman (1994).

We present a modification of the method in Rabczuk and Belytschko (2004). The major goal is to remove spurious cracking and simultaneously maintain the sim-

plicity of the method. This is accomplished by defining a set of cracking rules. Since spurious cracking occurs only at crack propagation, crack propagation has to be distinguished from crack nucleation. In other words, the cracking rules presented later are only used for propagating cracks. We show by some numerical experiments that we are able to capture complicated crack patterns. We also show that we are able to avoid spurious cracking and get convergence in the cohesive fracture energy even for complicated crack problems.

The paper is outlined as follows: We first describe the element-free Galerkin (EFG) method and the new cracking method. Then, the discrete equations are derived from the weak form. The cracking criterion and the cohesive model is described next. At the end, we will show three examples before we conclude our paper.

## 2 Element-free Galerkin method

The new cracking method is incorporated in a version of the element-free Galerkin (EFG) method Belytschko, Lu, and Gu (1994a). The EFG method is based on Moving Least Square (MLS) approximation written in terms of a polynomial basis  $\mathbf{p}(\mathbf{X})$  and unknown coefficients  $\mathbf{a}(\mathbf{X})$ :

$$\mathbf{u}^{con}(\mathbf{X}, t) = \sum_{I \in \mathcal{W}} p_I(\mathbf{X}) a_I(\mathbf{X}) = \mathbf{P}^T(\mathbf{X}) \mathbf{a}(\mathbf{X}) \quad (1)$$

where  $\mathcal{W}$  is the total set of nodes;  $\mathbf{p}^T(\mathbf{X}) = (1, X, Y)$ . Minimization of discrete weighted  $\mathcal{L}_2$  error norm  $E$  with respect to the unknown coefficients  $\mathbf{a}$

$$E = \sum_{I \in \mathcal{W}} (\mathbf{P}^T(\mathbf{X}_I) \mathbf{a}(\mathbf{X}_I) - \mathbf{u}_I)^2 w(\mathbf{X} - \mathbf{X}_I, h) \quad (2)$$

leads to the final EFG approximation

$$\mathbf{u}^{con}(\mathbf{X}, t) = \sum_{I \in \mathcal{W}} N_I(\mathbf{X}) \mathbf{u}_I(t) \quad (3)$$

with

$$N_I(\mathbf{X}) = \mathbf{p}^T(\mathbf{X}) A^{-1}(\mathbf{X}) \mathbf{D}_I(\mathbf{X}) \quad (4)$$

and

$$\begin{aligned} \mathbf{D}_I(\mathbf{X}) &= w(\mathbf{X} - \mathbf{X}_I, h) \mathbf{p}^T(\mathbf{X}_I) \\ \mathbf{A}_I(\mathbf{X}) &= \sum_{I \in \mathcal{W}} w(\mathbf{X} - \mathbf{X}_I, h) \mathbf{p}(\mathbf{X}_I) \mathbf{p}^T(\mathbf{X}_I) \end{aligned} \quad (5)$$

The superimposed *con* in eq. (3) denotes the continuous displacement field;  $w(\mathbf{X} - \mathbf{X}_I, h)$  is the weighting function and  $h$  is the interpolation radius of this weighting

function. For dynamic fracture, it is important to express the weighting function in term of material coordinates since kernel functions expressed in spatial coordinates can lead to instabilities and numerical fracture as shown by e.g. Belytschko, Guo, Liu, and Xiao (2000).

### 3 Displacement Field

Consider a displacement field which is continuous in the entire domain except at the crack where a discontinuity occurs in the displacement field. To describe this discontinuity, the displacement is decomposed into continuous and discontinuous parts:

$$\mathbf{u}(\mathbf{X}) = \underbrace{\mathbf{u}^{con}(\mathbf{X})}_{\text{continuous}} + \underbrace{\mathbf{u}^{dis}(\mathbf{X})}_{\text{discontinuous}} \quad (6)$$

In Rabczuk and Belytschko (2004), the crack is modeled by a set of discrete cracks that cross the entire domain of influence of a node. These discrete cracks are restricted to lie on a plane passing through this node, see figure 1. The major advantage is that no representation for the geometry of the crack is needed.

The approximation of the discontinuous displacement field is

$$\mathbf{u}^{dis}(\mathbf{X}) = \sum_{I \in \mathcal{W}_c} N_I(\mathbf{X}) H(\mathbf{X}) \mathbf{q}_I \quad (7)$$

where  $\mathcal{W}_c$  are the set of cracked nodes,  $\mathbf{q}_I$  are additional unknowns and  $H(\mathbf{X})$  is the step function that introduces the jump in the displacement field. Note that only

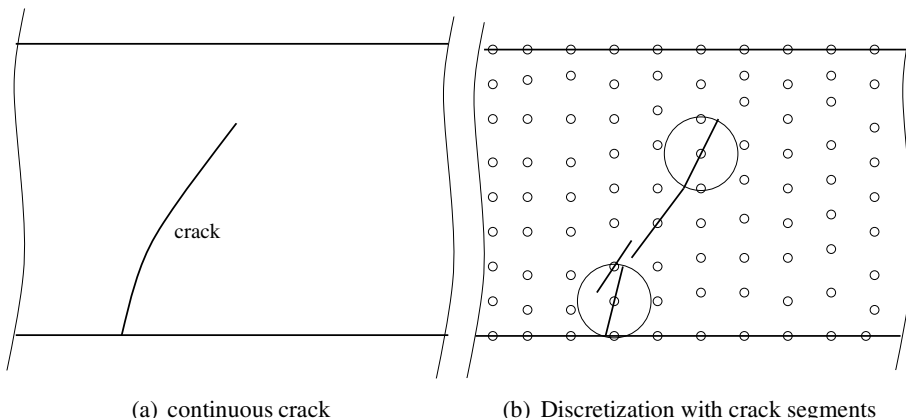


Figure 1: a) Continuous crack and b) representation of the crack with discrete cohesive crack segments

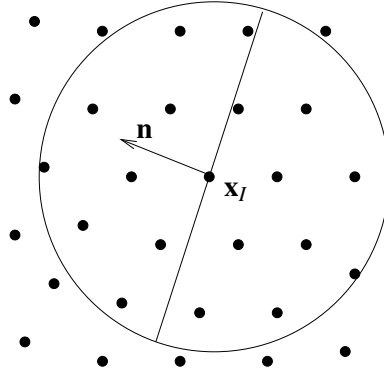


Figure 2: Normal of the crack segment

cracked nodes are enriched that significantly simplifies the implementation of the method. Only a small portion of the entire nodes are affected by the crack and the crack surface is entirely determined by the position vector of the cracked node and its normal that is obtained from the cracking criterion explained later, figure 2:

$$H(\mathbf{X}) = \begin{cases} 1 & \text{if } \mathbf{n} \cdot (\mathbf{X} - \mathbf{X}_I) > 0 \\ -1 & \text{if } \mathbf{n} \cdot (\mathbf{X} - \mathbf{X}_I) < 0 \end{cases} \quad (8)$$

The jump in the displacement field only depends on the additional unknowns  $\mathbf{q}$  and is given by

$$[[\mathbf{u}]](\mathbf{X}) = \sum_{I \in \mathcal{W}_c} 2 N_I(\mathbf{X}) \mathbf{q}_I \quad (9)$$

The test functions  $\delta\mathbf{u}$  have a similar structure:

$$\delta\mathbf{u}(\mathbf{X}) = \sum_{I \in \mathcal{W}} N_I(\mathbf{X}) \delta\mathbf{u}_I(t) + \sum_{I \in \mathcal{W}_c} N_I(\mathbf{X}) H(\mathbf{X}) \delta\mathbf{q}_I \quad (10)$$

As noted in the introduction, without further modification of the method, spurious crack nucleation is obtained when the crack propagates. This will be demonstrated later for some numerical examples. Therefore, we suggest the following modifications:

- A criterion is needed that distinguishes crack nucleation from crack propagation.
- A criterion is needed for crack branching.

- A criterion is needed to avoid spurious cracking.

Crack nucleation is distinguished from crack propagation by searching for existing cracked nodes in the vicinity of a newly inserted cracked node. The search domain is a circle of radius  $\alpha r_m$  with  $r_m$  being the interpolation radius of the weighting function and  $\alpha$  is a parameter. In all computations, the parameter  $\alpha$  is set to 1.2 though results did not significantly change for larger parameters of  $\alpha$ .

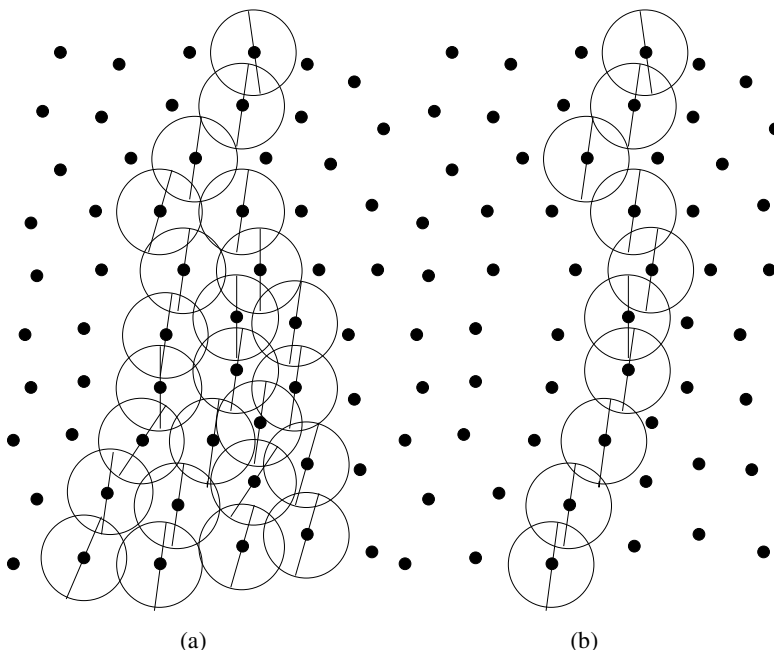


Figure 3: a) Spurious cracking during crack propagation and b) crack propagation without spurious cracking

Spurious cracking can occur adjacent to an existing crack, figure 3, or close to the crack tip, figure 4. The first type of spurious cracking is avoided by an exclusion zone that does not allow development of *parallel* cracks far away from the crack tip, figure 3. The crack tip is defined as the last cracked node for the case "crack propagation".

In most dynamic computations, cracking criterion is met at several material points around the crack tip due to similar stress states, figure 3. This can lead to branching cracks. Allowing only one node in front of the crack tip to crack avoids crack branching completely. Therefore, a criterion for crack branching has to be introduced first. A crack is assumed to branch if the angle between an existing crack

tip node and newly initiated cracks exceeds a certain value. Therefore, we compute deviation in the crack direction, figure 4:

$$\gamma_{\max} = \underbrace{\max}_{I \in \tilde{\mathcal{W}}_c} (\mathbf{n}_{ct} \cdot \mathbf{n}_I) \quad \forall I \in \tilde{\mathcal{W}}_c \quad (11)$$

$$\gamma_{\min} = \underbrace{\min}_{I \in \tilde{\mathcal{W}}_c} (\mathbf{n}_{ct} \cdot \mathbf{n}_I) \quad \forall I \in \tilde{\mathcal{W}}_c \quad (12)$$

where  $\tilde{\mathcal{W}}_c \subset \mathcal{W}_c$  is the set of newly cracked nodes, i.e. between time step  $n$  and time step  $n+1$ . If  $\gamma_{\max} - \gamma_{\min} \geq TOL$ , the crack branches. In the current implementation, we allow only two branches though this is not compulsory.

After deciding if crack branches or not, a criterion has to be implemented that avoids spurious cracking. Let  $K = 1$  or  $2$  denote the number of crack branches of an associated advancing crack. Then,  $K$  number of cracked nodes are introduced in front of an existing crack tip. The closest node(s) where the cracking criterion is met, will be cracked. If  $K = 2$ , two crack tips (of the original 1 crack) will exist in the next time step.

It is instructive to mention that generally cracking criterion is met at several material points under crack initiation. In this case, we also allow only one node to crack at a time. The position of the cracked node is obtained by an average procedure. The closest node to the averaged position vector of all nodes that meet cracking criterion is cracked.

#### 4 Weak Form and Discretization

The linear momentum equation is

$$\nabla \cdot \mathbf{P} + \rho \mathbf{b} = \rho \ddot{\mathbf{u}}, \quad \mathbf{X} \in \Omega \quad (13)$$

where  $\mathbf{P}$  is the nominal stress tensor,  $\rho$  is the density,  $\mathbf{b}$  are body forces and the superimposed dots denote material time derivatives. The displacement and traction boundary conditions are:

$$\mathbf{u} = \bar{\mathbf{u}}, \quad \mathbf{X} \in \Gamma_u \quad (14)$$

$$\mathbf{n}_t \cdot \mathbf{P} = \bar{\mathbf{t}}, \quad \mathbf{X} \in \Gamma_t \quad (15)$$

$$\mathbf{n}_c \cdot \mathbf{P} = \mathbf{t}_c([[\mathbf{u}]]) , \quad \mathbf{X} \in \Gamma_c \quad (16)$$

where the index  $c$  refers to the crack, the index  $t$  refers to traction boundaries and the index  $u$  refers to displacement boundaries. The weak form of the linear momentum

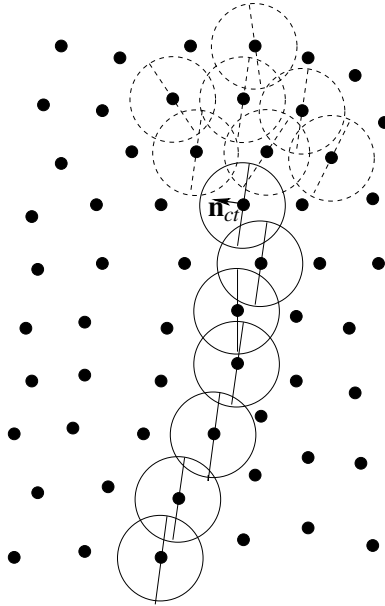


Figure 4: Crack with crack tip node (solid line) at time  $n$  and nodes that meet cracking criterion at time  $n + 1$  (dashed line)

equation is: Find  $\mathbf{u} \in \mathcal{U}$  and  $\delta\mathbf{u} \in \mathcal{U}_0$  such that

$$\delta W = \delta W_{int} - \delta W_{ext} + \delta W_{inertia} + \delta W_{coh} = 0 \quad (17)$$

with

$$\begin{aligned} \delta W_{int} &= \int_{\Omega} \nabla \delta \mathbf{u} : \mathbf{P} d\Omega \\ \delta W_{ext} &= \int_{\Gamma_t} \delta \mathbf{u} \cdot \bar{\mathbf{t}} d\Gamma + \int_{\Omega} \rho \delta \mathbf{u} \cdot \mathbf{b} d\Omega \\ \delta W_{inertia} &= \int_{\Omega} \rho \delta \mathbf{u} \cdot \ddot{\mathbf{u}} d\Omega \\ \delta W_{coh} &= \int_{\Gamma_c} \delta [[\mathbf{u}]] \cdot \mathbf{t}_c d\Gamma \end{aligned} \quad (18)$$

and  $\mathcal{U}$  and  $\mathcal{U}_0$  are the approximation spaces for the trial and test functions:

$$\begin{aligned} \mathcal{U} &= \{ \mathbf{u}(\mathbf{X}, t) | \mathbf{u} \in H^1, \mathbf{u} = \bar{\mathbf{u}} \text{ on } \Gamma_u, \mathbf{u} \text{ discontinuous on } \Gamma_c \} \\ \mathcal{U}_0 &= \{ \delta \mathbf{u} | \delta \mathbf{u} \in H^1, \delta \mathbf{u} = 0 \text{ on } \Gamma_u, \delta \mathbf{u} \text{ discontinuous on } \Gamma_c \} \end{aligned} \quad (19)$$

The discretized equations are obtained by substituting the test and trial functions into equation (17):

$$\begin{aligned} \sum_{J=1}^n \int_{\Omega_J} \nabla \delta \mathbf{u}_J : \mathbf{P} d\Omega - \sum_{J=1}^n \int_{\Gamma_{t,J}} \delta \mathbf{u} \cdot \bar{\mathbf{t}} d\Gamma - \sum_{J=1}^n \int_{\Omega_J} \rho \delta \mathbf{u} \cdot \mathbf{b} d\Omega \\ + \int_{\Gamma_{c,J}} \delta[[\mathbf{u}]] \cdot \mathbf{t}_c d\Gamma + \sum_{J=1}^n \int_{\Omega_J} \rho \delta \mathbf{u} \cdot \ddot{\mathbf{u}} d\Omega = 0 \end{aligned} \quad (20)$$

The final system of equations in matrix form is given by:

$$\begin{bmatrix} \mathbf{M}_{IJ}^{uu} & \mathbf{M}_{IJ}^{uq} \\ \mathbf{M}_{IJ}^{qu} & \mathbf{M}_{IJ}^{qq} \end{bmatrix} \cdot \begin{bmatrix} \ddot{\mathbf{u}}_J \\ \ddot{\mathbf{q}}_J \end{bmatrix} = \begin{bmatrix} \mathbf{f}_{I,ext}^u - \mathbf{f}_{I,int}^u \\ \mathbf{f}_{I,ext}^q - \mathbf{f}_{I,int}^q \end{bmatrix} \quad (21)$$

with

$$\mathbf{f}_{I,ext}^u = \int_{\Gamma_t} (\mathbf{N}_I^u)^T \mathbf{t} d\Gamma + \int_{\Omega} (\mathbf{N}_I^u)^T \mathbf{b} d\Omega \quad (22)$$

$$\begin{aligned} \mathbf{f}_{I,ext}^q &= \int_{\Gamma_t} (\mathbf{N}_I^q)^T \mathbf{t} d\Gamma + \int_{\Omega} (\mathbf{N}_I^q)^T \mathbf{b} d\Omega \\ &+ \int_{\Gamma_c} [[(\mathbf{N}_I^q)^T]] \mathbf{t}_c d\Gamma \text{ with } \mathbf{N}_I^q = \mathbf{N}_I \Psi(\mathbf{X}) \end{aligned} \quad (23)$$

$$\mathbf{f}_{I,int}^u = \int_{\Omega} (\mathbf{B}_I^u)^T \mathbf{P} d\Omega \quad (24)$$

$$\mathbf{f}_{I,int}^q = \int_{\Omega} (\mathbf{B}_I^q)^T \mathbf{P} d\Omega \text{ with } \mathbf{B}_I^q = \Psi(\mathbf{X}) \nabla \mathbf{N}_I \quad (25)$$

$$\begin{aligned} \mathbf{M}_{IJ}^{uu} &= \mathbf{M}_{IJ}^{qq} = \int_{\Omega} \rho \mathbf{N}_I \mathbf{N}_J^T d\Omega \\ \mathbf{M}_{IJ}^{uq} &= \mathbf{M}_{IJ}^{qu} = \int_{\Omega} \rho \Psi(\mathbf{X}) \mathbf{N}_I \mathbf{N}_J^T d\Omega \end{aligned} \quad (26)$$

The integrals are evaluated by stress point integration as explained detailed in Rabczuk and Belytschko (2004). We use explicit central difference time integration. To benefit from explicit time integration, one generally takes advantage of lumped mass matrix. However, in the presence of additional degrees of freedom  $\mathbf{q}$ , standard mass lumping might lead to negative masses.

F.L., Colominas, Moscaneira, Navarrina, and Casteleiro (2004) showed that the lumped mass matrix obtained via the volume of Voronoi cells ( $M = V \cdot \rho$  where

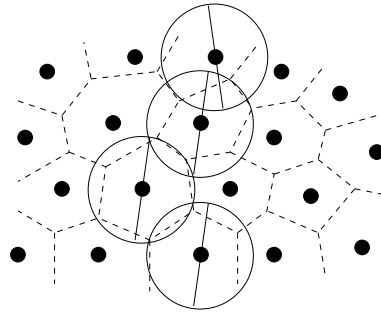


Figure 5: Cracked nodes with crack segments (solid lines) and Voronoi cells (dashed line)

$V$  is the volume of the Voronoi cell and  $\rho$  is the density of the material) is identical to lumped mass matrix from standard row-sum technique. We therefore build the lumped mass matrix from Voronoi cells. The mass of the (enriched) cracked node is modified according to its area ratio, figure 5. Results by this method were similar to the results obtained from using consistent mass matrix. Since the cracked node always lies in the middle of the associated Voronoi cell, figure 5, the critical time step is influenced only marginal. We use a Courant number of 0.5 and did not observe any instabilities.

## 5 Cracking criterion and cohesive law

Rankine criterion determines the onset of cracking and crack propagation. The crack is introduced perpendicular to the direction of the maximum principal stress. The traction acting across the crack surface are related to the jump in the displacement, equation (9). It can be decomposed into a normal and tangential part:

$$\delta_n = [[\mathbf{u}]] \cdot \mathbf{n} \quad (27)$$

$$\delta_t = |[[\mathbf{u}]]_s| = |[[\mathbf{u}]] - \delta_n \mathbf{n}| \quad (28)$$

We use the cohesive law proposed by Pandolfi, Krysl, and Ortiz (1999) that makes use of effective crack opening displacement

$$\delta = \sqrt{\beta^2 \delta_t^2 - \delta_n^2} \quad (29)$$

where the parameter  $\beta$  defines the ratio between tangential and normal critical traction. The effective traction-separation law is given by

$$t = \frac{t_{max}}{\delta_{max}} \delta \text{ if } \delta \leq \delta_{max} \text{ or } \dot{\delta} < 0 \quad (30)$$

The traction vector is then computed by

$$\mathbf{t} = \frac{t}{\delta} (\beta^2 [[\mathbf{u}]]_s + \delta_n \mathbf{n}) \quad (31)$$

More details are given in Pandolfi, Krysl, and Ortiz (1999).

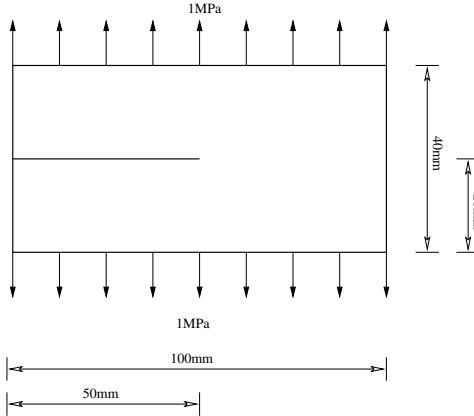


Figure 6: Plate with a horizontal initial notch under tensile tractions

## 6 Results

### 6.1 Crack branching

The first example is the pre-notched specimen under tensile loading,  $\sigma = 1MPa$ , shown in figure 6. Numerical results for this problem are reported in Xu and Needleman (1994) and experimental results with different dimensions are available in Ravi-Chandar (1998); Sharon, Gross, and Fineberg (1995); Fineberg, Sharon, and Cohen (2003). The Young's modulus is  $E = 32,000MPa$  and Poisson's ratio is  $\nu = 0.20$ . The initial Rayleigh wave speed is  $c_R = 2119.0m/s$ . This problem is studied with different refinements. The tolerance angle deciding about crack branching was 30 degree. We also studied this problem without the set of cracking rules proposed in the previous sections.

The pattern of crack propagation at different stages of the simulation is shown in figure 7. Without avoiding spurious cracking, the crack pattern is fringy and the width of the crack varies. These observations agree with the results in Rabczuk and Belytschko (2004). The speed of the crack tip is shown in figure 8. The spurious cracks do not seem to have any influence on the crack speed. This suggests that

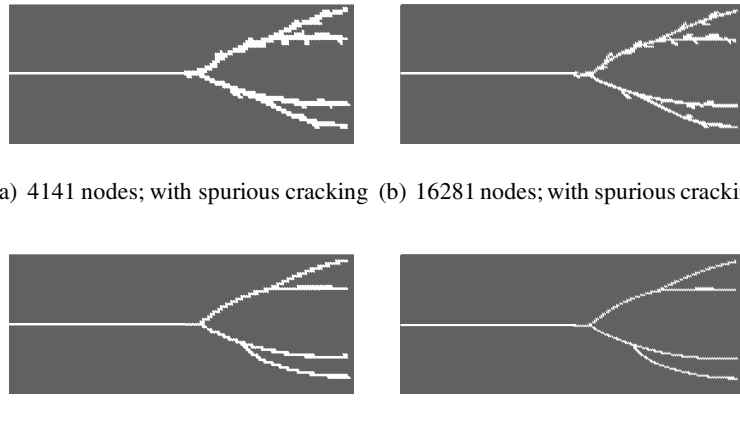


Figure 7: Crack pattern for the crack branching problem

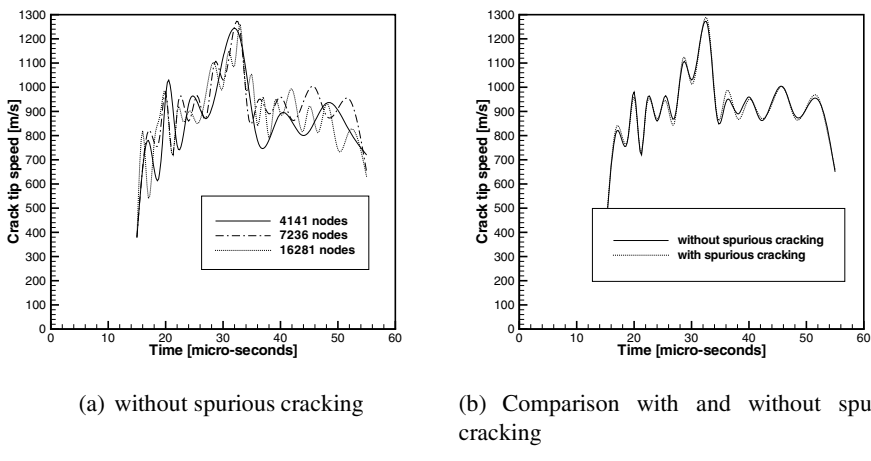


Figure 8: Crack tip speed for the crack branching problem

the spurious cracks occur adjacent to the crack far away from the crack tip. We also observe increase in the crack speed before the crack branches. Afterwards, the crack speed decreases. This is in agreement with results reported by other authors Sharon, Gross, and Fineberg (1995); Fineberg, Sharon, and Cohen (2003); Ravi-Chandar (1998).

The cohesive fracture energy is reported in figure 9. It is lower when spurious cracking is avoided. The cohesive fracture energy diverges or converges very slowly when spurious cracking is not suppressed.

## 6.2 Kalthoff experiment

JF and Winkler (1987) reported experimental results in which a plate with two initial edge notches is impacted by a projectile. The experimental set-up is shown in figure 10. The impact velocity is  $20m/s$ . In the experiment, a crack propagated with angle of about 70 degrees versus the horizontal axis. We study this problem. Only the upper part of the plate is modeled due to symmetry. The material properties of the steel used in the experiment JF (2000) are Young's modulus  $E = 190GPa$ , density  $\rho = 8000kg/m^3$  and Poisson's ratio  $\nu = 0.3$ . The crack path at the end of the simulation is illustrated in figure 11 and agrees well with the experimental results. The crack speed is shown in figure 12a. It is not influenced by spurious cracking. However, the cohesive fracture energy is significantly higher when spurious cracking is not suppressed, figure 12.

## 7 Conclusions

We presented a set of cracking rules to avoid spurious cracking in a simplified meshless method with embedded discontinuities. The simplified method is based on local partition of unity and introduces discrete cracks at nodes. The crack is represented by a set of discrete cracked nodes. No representation of crack surface is needed that makes the method appealing for many cracks.

We showed that the method can handle complicated problems with many cracks and also branching cracks. We showed improvements in the crack pattern and showed that with the cracking rules, convergence in the cohesive fracture energy is obtained.

## References

- Andreaus, U.; Batra, B.; Porfiri, M.** (2005): Vibrations of cracked euler-bernoulli beams using meshless local petrov-galerkin (mlpg) method. *CMES-Computer Modeling in Engineering & Sciences*, vol. 9, pp. 111–131.

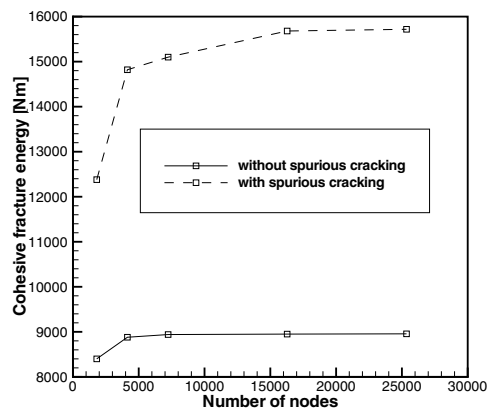


Figure 9: Cohesive fracture energy of the branching crack problem

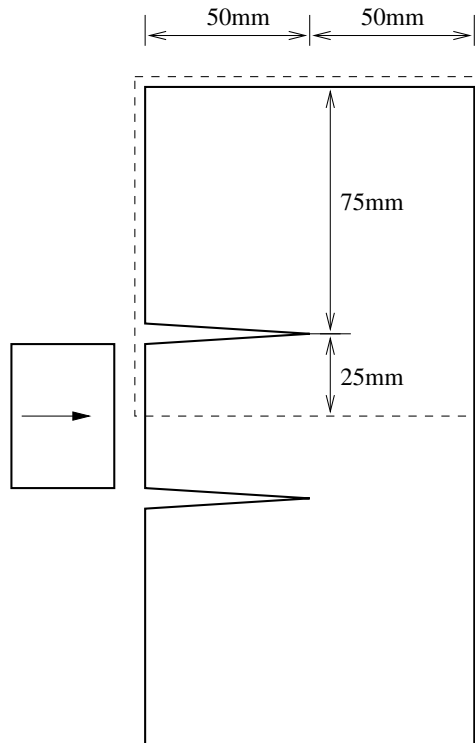


Figure 10: Kalthoff problem

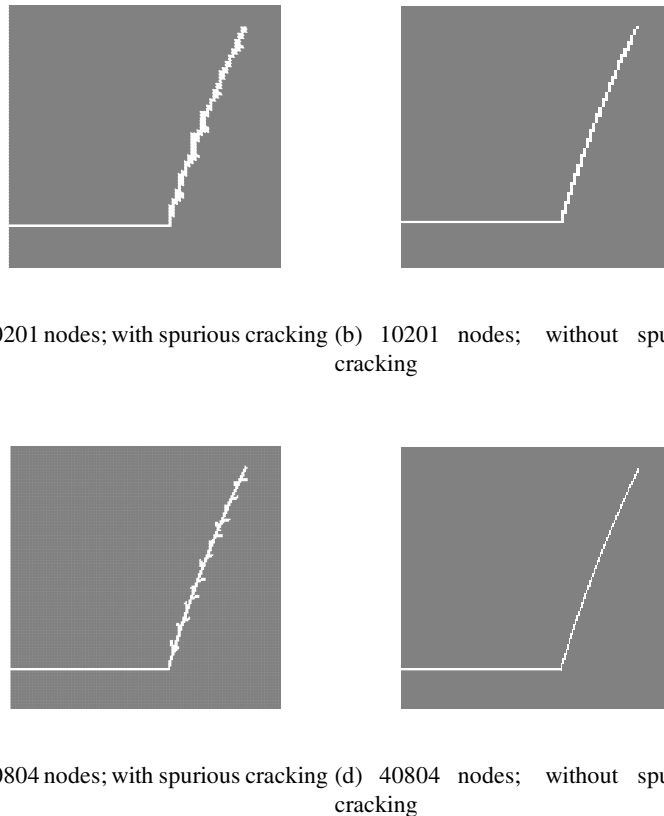


Figure 11: Final crack path of the Kalthoff problem

**Atluri, S.** (2002): *The Meshless Local Petrov-Galerkin (MLPG) Method*. Tech Science Press.

**Atluri, S.; Shen, S.** (2002): The meshless local petrov-galerkin method: a simple and less-costly alternative to the finite element and boundary element methods. *Computations and Modelling in Engineering and Sciences*, vol. 3, pp. 11–51.

**Atluri, S.; Zhu, T.** (1998): A new meshless local petrov-galerkin (mlpg) approach in computational mechanics. *Computational Mechanics*, vol. 22, pp. 117–127.

**Atluri, S.; Zhu, T.** (2000): The meshless local petrov-galerkin (mlpg) approach for solving problems in elasto-statics. *Computational Mechanics*, vol. 25, pp. 169–179.

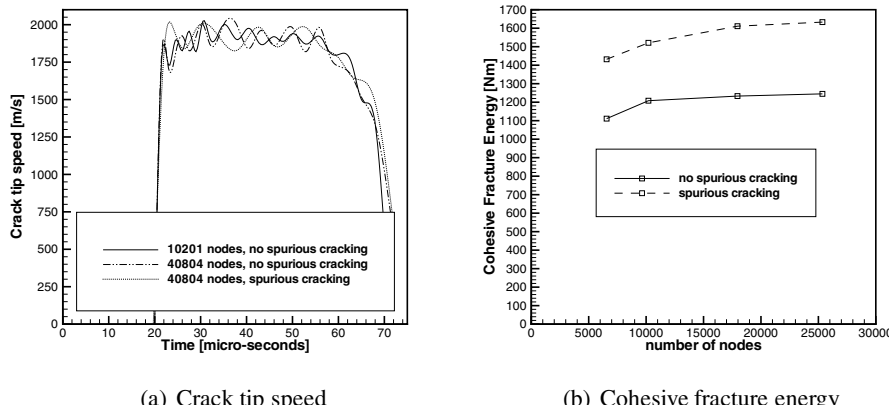


Figure 12: Crack tip speed and cohesive fracture energy of the Kalthoff problem

**Belytschko, T.; Fleming, M.** (1999): Smoothing, enrichment and contact in the element free galerkin method. *Computers & Structures*, vol. 71, pp. 173–195.

**Belytschko, T.; Guo, Y.; Liu, W.; Xiao, S.** (2000): A unified stability analysis of meshfree particle methods. *International Journal for Numerical Methods in Engineering*, vol. 48, pp. 1359–1400.

**Belytschko, T.; Lu, Y.** (1995): Element-free galerkin methods for static and dynamic fracture. *International Journal of Solids and Structures*, vol. 32, pp. 2547–2570.

**Belytschko, T.; Lu, Y.; Gu, L.** (1994): Element-free galerkin methods. *International Journal for Numerical Methods in Engineering*, vol. 37, pp. 229–256.

**Belytschko, T.; Lu, Y.; Gu, L.** (1994): Element-free galerkin methods. *International Journal for Numerical Methods in Engineering*, vol. 37, pp. 229–256.

**Belytschko, T.; Lu, Y.; Gu, L.** (1995): Crack propagation by element-free galerkin methods. *Engineering Fracture Mechanics*, vol. 51, no. 2, pp. 295–315.

**Belytschko, T.; Tabbara, M.** (1996): Dynamic fracture using element-free galerkin methods. *International Journal for Numerical Methods in Engineering*, vol. 39, no. 6, pp. 923–938.

**Chen, W.; Chen, C.** (2005): On three-dimensional fracture mechanics analysis by an enriched meshless method. *CMES-Computer Modeling in Engineering & Sciences*, vol. 8, no. 3, pp. 177–190.

**Chen, Z.; Gan, Y.; Chen, J.** (2008): A coupled thermo-mechanical model for simulating the material failure evolution due to localized heating. *CMES-Computer Modeling in Engineering & Sciences*, vol. 26, no. 2, pp. 123–137.

**Fineberg, J.; Sharon, E.; Cohen, G.** (2003): Crack front waves in dynamic fracture. *International Journal of Fracture*, vol. 121, pp. 55–69.

**F.L., C.; Colominas, I.; Mosqueira, G.; Navarrina, F.; Casteleiro, M.** (2004): On the galerkin formulation of smoothed particle hydrodynamics. *International Journal for Numerical Methods in Engineering*, vol. 60, pp. 1475–1512.

**Fujimoto, T.; Nishioka, T.** (2006): Numerical simulation of dynamic elasto visco-plastic fracture using moving finite element method. *CMES-Computer Modeling in Engineering & Sciences*, vol. 11, no. 2, pp. 91–101.

**Gao, L.; Liu, K.; Liu, Y.** (2006): Applications of mlpg method in dynamic fracture problems. *CMES-Computer Modeling in Engineering & Sciences*, vol. 12, no. 3, pp. 181–195.

**Gao, L.; Liu, K.; Liu, Y.** (2006): Applications of mlpg method in dynamic fracture problems. *CMES-Computer Modeling in Engineering & Sciences*, vol. 12, no. 3, pp. 181–195.

**Guo, Y.; Nairn, J.** (2006): Three-dimensional dynamic fracture analysis using the material point method. *CMES-Computer Modeling in Engineering & Sciences*, vol. 16, no. 3, pp. 141–155.

**Guo, Y.; Nairn, J.** (2006): Three-dimensional dynamic fracture analysis using the material point method. *CMES-Computer Modeling in Engineering & Sciences*, vol. 16, no. 3, pp. 141–155.

**Guz, A.; Menshykov, O.; Zozulya, V.** (2007): Contact problem for the flat elliptical crack under normally incident shear wave. *CMES-Computer Modeling in Engineering & Sciences*, vol. 17, no. 3, pp. 205–214.

**Hagihara, S.; Tsunori, M.; Ikeda, T.** (2007): Application of meshfree method to elastic-plastic fracture mechanics parameter analysis. *CMES-Computer Modeling in Engineering & Sciences*, vol. 17, no. 2, pp. 63–72.

**Han, Z.; Atluri, S.** (2004): A meshless local petrov-galerkin (mlpg) approach for 3-dimensional elasto-dynamics. *CMC-Computers Materials & Continua*, vol. 2, no. 1, pp. 129–140.

**Hao, S.; Liu, W.** (2006): Moving particle finite element method with superconvergence: Nodal integration formulation and applications. *Computer Methods in Applied Mechanics and Engineering*, vol. 195, no. 44-47, pp. 6059–6072.

**Hao, S.; Liu, W.; Chang, C.** (2000): Computer implementation of damage models by finite element and meshfree methods. *Computer Methods in Applied Mechanics and Engineering*, vol. 187, no. 3-4, pp. 401–440.

**Hao, s.; Liu, W.; Klein, P.; Rosakis, A.** (2004): Modeling and simulation of intersonic crack growth. *International Journal of Solids and Structures*, vol. 41, no. 7, pp. 1773–1799.

**Hao, S.; Liu, W.; Qian, D.** (2000): Localization-induced band and cohesive model. *Journal of Applied Mechanics-Transactions of the ASME*, vol. 67, no. 4, pp. 803–812.

**Idelsohn, S.; Onate, E.; Pin, F. D.** (2004): The particle finite element method: a powerful tool to solve incompressible flows with free surfaces and breaking waves. *International Journal for Numerical Methods in Engineering*, vol. 61, pp. 964–989.

**JF, K.** (2000): Modes of dynamic shear failure in solids. *International Journal of Fracture*, vol. 101, pp. 1–31.

**JF, K.; Winkler, S.** (1987): Failure mode transition at high rates of shear loading. *International Conference on Impact Loading and Dynamic Behavior of Materials*, vol. 1, pp. 185–195.

**Le, P.; Mai-Duy, N.; Tran-Cong, T.** (2008): A meshless modeling of dynamic strain localization in quasi-brittle materials using radial basis function networks. *CMES-Computer Modeling in Engineering & Sciences*, vol. 25, no. 1, pp. 43–67.

**Liu, K.; Long, S.; Li, G.** (2008): A meshless local petrov-galerkin method for the analysis of cracks in the isotropic functionally graded material. *CMC-Computers Materials & Continua*, vol. 7, no. 1, pp. 43–57.

**Liu, W.; Hao, S.; Belytschko, T.** (1999): Multiple scale meshfree methods for damage fracture and localization. *Computational Material Science*, vol. 16, no. 1-4, pp. 197–205.

**Liu, W.; Jun, S.; Zhang, Y.** (1995): Reproducing kernel particle methods. *International Journal for Numerical Methods in Engineering*, vol. 20, pp. 1081–1106.

**Ma, J.; Lu, H.; Wang, B.** (2006): Multiscale simulation using generalized interpolation material point (gimp) method and molecular dynamics (md). *CMES-Computer Modeling in Engineering & Sciences*, vol. 14, no. 2, pp. 101–117.

- Macri, M.; De, S.** (2008): An octree partition of unity method (octpum) with enrichments for multiscale modeling of heterogeneous media. *Computers & Structures*, vol. 86, no. 7-8, pp. 780–795.
- Mai-Duy, N.; Khennane, A.; Tran-Cong, T.** (2007): Computation of laminated composite plates using integrated radial basis function networks. *CMC-Computers Materials & Continua*, vol. 5, no. 1, pp. 63–77.
- Maiti, S.; Geubelle, P.** (2004): Mesoscale modeling of dynamic fracture of ceramic materials. *CMES-Computer Modeling in Engineering & Sciences*, vol. 5, no. 2, pp. 91–101.
- Miers LS, T. J.** (2006): On the ngf procedure for libe elastostatic fracture mechanics. *CMES-Computer Modeling in Engineering & Sciences*, vol. 14, no. 3, pp. 161–169.
- Nairn, J.** (2003): Material point method calculations with explicit cracks. *CMES-Computer Modeling in Engineering & Sciences*, vol. 4, no. 6, pp. 649–663.
- Nguyen-Van, H.; N, N. M.-D.; Tran-Cong, T.** (2008): A smoothed four-node piezoelectric element for analysis of two-dimensional smart structures. *CMES-Computer Modeling in Engineering & Sciences*, vol. 23, no. 3, pp. 209–222.
- Nishioka, T.** (2005): Recent advances in numerical simulation technologies for various dynamic fracture phenomena. *CMES-Computer Modeling in Engineering & Sciences*, vol. 10, no. 3, pp. 209–215.
- Nishioka, T.; Kobayashi, Y.; Fujimoto, T.** (2007): The moving finite element method based on delaunay automatic triangulation for fracture path prediction simulations in nonlinear elastic-plastic materials. *CMES-Computer Modeling in Engineering & Sciences*, vol. 17, no. 3, pp. 231–238.
- Nishioka, T.; Tchouikov, S.; Fujimoto, T.** (2006): Numerical investigation of the multiple dynamic crack branching phenomena. *CMC-Computers Materials & Continua*, vol. 3, no. 3, pp. 147–153.
- Organ, D.; Fleming, M.; Terry, T.; Belytschko, T.** (1996): Continuous meshless approximations for nonconvex bodies by diffraction and transparency. *Computational Mechanics*, vol. 18, pp. 225–235.
- Ortiz, M.; Leroy, Y.; Needleman, A.** (1987): Finite element method for localized failure analysis. *Computer Methods in Applied Mechanics and Engineering*, vol. 61, pp. 189–213.

**Ostachowicz, W.** (2008): Damage detection of structures using spectral finite element method. *Computers & Structures*, vol. 86, pp. 454–462.

**Pandolfi, A.; Krysl, P.; Ortiz, M.** (1999): Finite element simulation of ring expansion and fragmentation: The capturing of length and time scales through cohesive models of fracture. *International Journal of Fracture*, vol. 95, pp. 279–297.

**Rabczuk, T.; Areias, P.** (2006): A meshfree thin shell for arbitrary evolving cracks based on an extrinsic basis. *CMES-Computer Modeling in Engineering & Sciences*, vol. 16, no. 2, pp. 115–130.

**Rabczuk, T.; Areias, P.** (2006): A meshfree thin shell for arbitrary evolving cracks based on an extrinsic basis. *CMES-Computer Modeling in Engineering & Sciences*, vol. 16, no. 2, pp. 115–130.

**Rabczuk, T.; Areias, P.; Belytschko, T.** (2007): A meshfree thin shell method for non-linear dynamic fracture. *International Journal for Numerical Methods in Engineering*, vol. 72, no. 5, pp. 524–548.

**Rabczuk, T.; Belytschko, T.** (2004): Cracking particles: A simplified mesh-free method for arbitrary evolving cracks. *International Journal for Numerical Methods in Engineering*, vol. 61, no. 13, pp. 2316–2343.

**Rabczuk, T.; Belytschko, T.** (2005): Adaptivity for structured meshfree particle methods in 2d and 3d. *International Journal for Numerical Methods in Engineering*, vol. 63, no. 11, pp. 1559–1582.

**Rabczuk, T.; Belytschko, T.** (2006): Application of particle methods to static fracture of reinforced concrete structures. *International Journal of Fracture*, vol. 137, no. 1-4, pp. 19–49.

**Rabczuk, T.; Belytschko, T.** (2007): A three dimensional large deformation meshfree method for arbitrary evolving cracks. *Computer Methods in Applied Mechanics and Engineering*, vol. 196, pp. 2777–2799.

**Rabczuk, T.; Belytschko, T.; Xiao, S.** (2004): Stable particle methods based on lagrangian kernels. *Computer Methods in Applied Mechanics and Engineering*, vol. 193, pp. 1035–1063.

**Rabczuk, T.; PMA, P. A.; Belytschko, T.** (2007): A simplified mesh-free method for shear bands with cohesive surfaces. *International Journal for Numerical Methods in Engineering*, vol. 69, no. 5, pp. 993–1021.

- Rabczuk, T.; Zi, G.** (2007): A meshfree method based on the local partition of unity for cohesive cracks. *Computational Mechanics*, vol. 39, no. 6, pp. 743–760.
- Ravi-Chandar, K.** (1998): Dynamic fracture of nominally brittle materials. *International Journal of Fracture*, vol. 90, pp. 83–102.
- Sharon, E.; Gross, P.; Fineberg, J.** (1995): Local crack branching as a mechanism for instability in dynamic fracture. *Physical Review Letters*, vol. 74, pp. 5096–5099.
- Sladek, J.; Sladek, V.; Krivacek, J.** (2005): Meshless local petrov-galerkin method for stress and crack analysis in 3-d axisymmetric fgm bodies. *CMES-Computer Modeling in Engineering & Sciences*, vol. 8, no. 3, pp. 259–270.
- Sladek, J.; Sladek, V.; Zhang, C.** (2007): Fracture analyses in continuously nonhomogeneous piezoelectric solids by the mlpg. *CMES-Computer Modeling in Engineering & Sciences*, vol. 19, no. 3, pp. 247–262.
- Sladek, J.; V. Sladek, V.; Zhang, C.** (2007): Application of the mlpg to thermo-piezoelectricity. *CMES-Computer Modeling in Engineering & Sciences*, vol. 22, pp. 217–233.
- Vavourakis, V.; Polyzos, D.** (2007): A mlpg4 (lbie) formulation in elastostatics. *CMC-Computer Materelas & Continua*, vol. 5, no. 3, pp. 185–196.
- Ventura, G.; Xu, J.; Belytschko, T.** (2002): A vector level set method and new discontinuity approximation for crack growth by efg. *International Journal for Numerical Methods in Engineering*, vol. 54, no. 6, pp. 923–944.
- Volokh, K.** (2004): Comparison between cohesive zone models. *Communications in Numerical Methods in Engineering*, vol. 20, no. 11, pp. 845–856.
- Wen, P.; Aliabadi, M.; Lin, Y.** (2008): Meshless method for crack analysis in functionally graded materials with enriched radial base functions. *CMES-Computer Modeling in Engineering & Sciences*, vol. 30, no. 3, pp. 133–147.
- Wen, P.; Hon, Y.** (2007): Geometrically nonlinear analysis of reissner-mindlin plate by meshless computation. *CMES-Computer Modeling in Engineering & Sciences*, vol. 21, pp. 177–191.
- Wu, C.; Liu, K.** (2007): A state space approach for the analysis of doubly curved functionally graded elastic and piezoelectric shells. *CMC-Computers Materials & Continua*, vol. 6, no. 3, pp. 177–199.

**Wu, X.; Tao, S. S. W.** (2007): Meshless local petrov-galerkin collocation method for two-dimensional heat conduction problems. *CMES-Computer Modeling in Engineering & Sciences*, vol. 22, pp. 65–76.

**Xu, S.; Dong, Y.; Zhang, Y.** (2008): An efficient model for crack propagation. *CMES-Computer Modeling in Engineering & Sciences*, vol. 30, no. 1, pp. 17–26.

**Xu, X.-P.; Needleman, A.** (1994): Numerical simulations of fast crack growth in brittle solids. *Journal of the Mechanics and Physics of Solids*, vol. 42, pp. 1397–1434.

**Zi, G.; Rabczuk, T.; Wall, W.** (2007): Extended meshfree methods without branch enrichment for cohesive cracks. *Computational Mechanics*, vol. 40, no. 2, pp. 367–382.